

# Cl<sup>-</sup> Absorption across the Thick Ascending Limb Is Not Altered in Cystic Fibrosis Mice

## A Role for a Pseudo-CFTR Cl<sup>-</sup> Channel

Pedro Marvão,\* Marie-Céleste De Jesus Ferreira,<sup>§</sup> Claire Bailly,<sup>§</sup> Marc Paulais,\* Marcelle Bens,<sup>‡</sup> Romain Guinamard,\* Richard Moreau,<sup>\*||</sup> Alain Vandewalle,<sup>‡</sup> and Jacques Teulon\*

\*INSERM CJF 95-07 and <sup>‡</sup>INSERM U478, Institut Fédératif de Recherche 02, Faculté de Médecine Xavier Bichat, Paris, France; <sup>§</sup>CNRS URA 1859, Centre d'Études Nucléaires de Saclay, Gif-sur-Yvette, France; and <sup>||</sup>INSERM U24, Hôpital Beaujon, Clichy, France

### Abstract

The cortical thick ascending limb (CTAL) absorbs Cl<sup>-</sup> via a Na<sup>+</sup>-K<sup>+</sup>-Cl<sup>-</sup> cotransport at the apical membrane and several Cl<sup>-</sup> channels at the basolateral membrane, including a 9-pS channel having several properties of the cystic fibrosis transmembrane conductance regulator (CFTR). Having checked that CFTR mRNA is present in the mouse CTAL, we investigated whether this channel is a CFTR molecule by applying the patch-clamp technique to CTALs microdissected from CFTR knockout mice (*cfr<sup>m1Unc</sup>*). The 9-pS channel was active in cell-attached patches from tubules of mice homozygous for the disrupted *cfr* gene [CFTR (-/-)] at the same frequency and with the same activity (NP<sub>o</sub>) as in normal [CFTR (+/+)] or heterozygous [CFTR (+/-)] mice. The conductive properties of the channel, studied on inside-out patches, were identical in CFTR (-/-), CFTR (+/+), and CFTR (+/-) tubules, as were the sensitivities to internal pH and internal ATP, two typical features of this channel. In addition, the Cl<sup>-</sup> absorption in isolated, microperfused CTALs and the Na<sup>+</sup>-K<sup>+</sup>-Cl<sup>-</sup> cotransport activity were identical in CFTR (-/-), CFTR (+/+), and CFTR (+/-) mice. These results show that the 9-pS Cl<sup>-</sup> channel is distinct from CFTR, and that the CFTR protein has no influence on the Cl<sup>-</sup> absorption in this part of the renal tubule. (*J. Clin. Invest.* 1998. 102:1986–1993.) Key words: Cl<sup>-</sup> channel • CFTR • basolateral membrane • kidney • epithelium

### Introduction

The thick ascending limb of the loop of Henle (TAL)<sup>1</sup> reabsorbs some 20–40% of the NaCl filtered by the glomerulus, mainly by the operation of a Na<sup>+</sup>-K<sup>+</sup>-2Cl<sup>-</sup> cotransporter at the

apical membrane, and Na<sup>+</sup>-K<sup>+</sup>-ATPase and Cl<sup>-</sup> conductance at the basolateral membrane (1). Studies on isolated, microperfused TALs have shown that the NaCl basal reabsorption occurring in this renal segment is increased two- to fivefold by several polypeptide hormones, including arginine vasopressin (AVP), acting via cAMP (1). This type of ion transport system is reminiscent of that used by Cl<sup>-</sup>-secreting epithelia such as the intestine and airways (2), where a Na<sup>+</sup>-K<sup>+</sup>-2Cl<sup>-</sup> cotransporter is located at the basolateral side of the epithelium (instead of the apical one), and there is an apical Cl<sup>-</sup> conductance (instead of a basolateral one). It is now clear that the cystic fibrosis transmembrane conductance regulator (CFTR) protein, in the epithelia where Cl<sup>-</sup> secretion is controlled by cAMP, is the Cl<sup>-</sup> channel mediating the apical membrane step of Cl<sup>-</sup> secretion (2).

We have shown recently that the Cl<sup>-</sup>-absorbing TAL of mouse kidney contains, in addition to the 20–40-pS Cl<sup>-</sup> channel found by us and others (3, 4), a 9-pS Cl<sup>-</sup> channel in the basolateral membrane that resembles the CFTR in several respects (5). This channel is active in the basal state and is stimulated by cAMP via phosphorylation. Like CFTR, the channel is stimulated by intracellular ATP in the presence of Mg<sup>2+</sup> and blocked by 5-nitro-2-(3-phenylpropylamino)benzoic acid and diphenylamine-2-carboxylic acid (5), but unlike CFTR (6, 7) it is very sensitive to internal pH (8). Several studies have shown that CFTR mRNA is present in all parts of the human and rat renal tubules, including the loop of Henle (9), and in the mouse kidney (10). Thus, the TAL 9-pS channel may be a CFTR molecule that is located at the basolateral side of TAL cells because of the absorptive function of this epithelium. Alternatively, this channel may be a distinct molecular entity, although it bears some functional resemblance to CFTR, and is the equivalent of CFTR for this type of epithelium, which absorbs Cl<sup>-</sup> under the control of cAMP.

This study was carried out to investigate this question in the cortical TAL by taking advantage of the recent creation of mice with a disrupted *CFTR* gene. We used the animal model created by Snouwaert et al. (10) by inserting a *neomycin* gene in place of part of exon 10 (*cfr<sup>m1Unc</sup>* mouse). Electrophysiological studies (11–15) demonstrated no cAMP-dependent Cl<sup>-</sup> secretion in jejunum, cecum, colon, nasal, and oviduct tissues of mice homozygous for the disrupted *cfr* gene. These mice suffer from a mild disorder of the pancreas and airways (14), due to the presence of an alternative secretory Cl<sup>-</sup> pathway, a calcium-sensitive Cl<sup>-</sup> channel which compensates for the total lack of cAMP-dependent Cl<sup>-</sup> currents (14, 15).

### Methods

This study used *cfr<sup>m1Unc</sup>* mice (10, 11) bred in the Centre de Développement des Techniques Avancées pour l'Expérimentation Ani-

Address correspondence to J. Teulon, INSERM CJF 95-07, Faculté Xavier Bichat, 16, rue Henri Huchard B.P. 416, 75870 Paris cedex 18, France. Phone: 33-1-44-85-62-61; FAX: 33-1-42-28-15-64; E-mail: teulon@bichat.inserm.fr

Received for publication 21 May 1998 and accepted in revised form 6 October 1998.

1. Abbreviations used in this paper: AVP, arginine vasopressin; CFTR, cystic fibrosis transmembrane conductance regulator; CTAL, cortical thick ascending limb of the nephron; EBCR, epithelial basolateral chloride conductance regulator; pH<sub>i</sub>, intracellular pH; TAL, thick ascending limb of the nephron.

J. Clin. Invest.

© The American Society for Clinical Investigation, Inc.  
0021-9738/98/12/1986/08 \$2.00

Volume 102, Number 11, December 1998, 1986–1993  
<http://www.jci.org>

male (CDTA, Orléans, France), and then delivered to the laboratory where experiments were done within a few days. Mice homozygous and heterozygous for the disrupted *CFTR* gene are referred to as *CFTR* ( $-/-$ ) and *CFTR* ( $+/-$ ) mice, respectively, while wild-type animals are *CFTR* ( $+/+$ ) mice. Male and female mice, aged 3–8 wk, were killed by cervical dislocation. *CFTR* ( $-/-$ ) mice ( $11.4 \pm 0.5$  g body wt,  $n = 40$ ) were considerably smaller than *CFTR* ( $+/+$ ) ( $17.9 \pm 0.6$  g body wt,  $n = 36$ ) and *CFTR* ( $+/-$ ) ( $19.0 \pm 0.6$  g body wt,  $n = 40$ ) mice ( $P < 0.05$ ). The genotype of each mouse was determined by PCR analysis of DNA using fragments of tail.

Short-circuit current experiments were done on distal colon tissues to verify that there was no cAMP-dependent  $\text{Cl}^-$  secretion in *CFTR* ( $-/-$ ) mice (11, 14). Tissues were bathed on both sides with an oxygenated Krebs solution containing  $\text{HCO}_3^-$ . Bilateral addition of  $10^{-5}$  M forskolin elicited no increase in short-circuit current ( $\Delta I_{sc}$ ) in *CFTR* ( $-/-$ ) mice ( $\Delta I_{sc} = -2.1 \pm 6.8 \mu\text{A}/\text{cm}^2$ ,  $n = 10$ ), whereas it significantly increased short-circuit current in *CFTR* ( $+/+$ ) mice ( $\Delta I_{sc} = -29.4 \pm 8.1 \mu\text{A}/\text{cm}^2$ ,  $n = 7$ ) and *CFTR* ( $+/-$ ) mice ( $\Delta I_{sc} = -19.6 \pm 6.0 \mu\text{A}/\text{cm}^2$ ,  $n = 11$ ).

**RT-PCR analysis.** Total RNA was extracted from whole mouse kidneys and microdissected mouse cortical thick ascending limbs of the nephron (CTALs) and was reverse-transcribed (16). 100–300 ng kidney cDNA, non-reverse-transcribed RNA, and CTAL cDNA were amplified for 34–35 cycles in a 100- $\mu\text{l}$  total volume containing 50 mM KCl, 20 mM Tris-HCl (pH 8.4), 40  $\mu\text{M}$  dNTP, 1.5 mM  $\text{MgCl}_2$ , 1 U *Taq* DNA polymerase, 42.6 pmol of *CFTR* primers, and 7.2 or 0.6 pmol  $\beta$ -actin primers, without or with 1  $\mu\text{Ci}$  [ $\alpha$ - $^{32}\text{P}$ ]dCTP. The two *CFTR* primers were: sense 5'-CAGTCATCTCTGCCTTGTGGGA-3' in the mouse *CFTR* exon 9 and antisense 5'-CGAACTGAGCTCGGACGTAGACT-3' in the mouse *CFTR* exon 13.  $\beta$ -actin primers were the same as described previously (16). The thermal cycling program was as follows: 94°C for 30 s, 60°C for 30 s, and 72°C for 60 s. Amplification products were run on 2% agarose gel, stained with ethidium bromide and photographed, or on 4% polyacrylamide gel and autoradiographed.

**Patch-clamp.** CTALs were microdissected from the mouse kidneys after a collagenase treatment (Worthington CLS II, 300 U/ml) as described previously (5). Two patch-clamp experiments were usually done simultaneously. Single-channel currents were recorded from patches of basolateral membranes using the cell-attached and inside-out configurations (17). The bath reference was 0.5 M KCl (in a 4% agar bridge) connected to an Ag/AgCl pellet. The applied clamp potential ( $V_c = V_{\text{bath}} - V_{\text{pipette}}$ ) is superimposed on the spontaneous cell membrane potential  $E_m$  (which is unknown) in cell-attached patches, while it corresponds to the *trans*-membrane potential in excised patches. Currents due to anions moving from the outer to the inner surface of the patch are positive and correspond to upward deflections in single-channel current tracings.

Single-channel current recordings were filtered at 300 Hz, digitized at 1 kHz, and analyzed with custom-designed software (Thierry Van den Abbeele, Paris, France). The normalized currents ( $NP_o$ ) were calculated from the equation  $I = NP_o i$ , where  $i$  is the amplitude of the unit current of the 9-pS channel. The mean current ( $I$ ) passing through the channels present in the patch was estimated from current amplitude histograms, taking the closed current level for the 9-pS channel as reference. In cell-attached patches, the closed current level was determined by inhibiting the pH-sensitive 9-pS channel by  $\text{NH}_4\text{Cl}$  superfusion. Other channels contributed minimally to the total current. The large-conductance  $\text{Cl}^-$  channel (3) generally had a low activity. A few measurements which showed highly active high-conductance  $\text{Cl}^-$  channels were not included in the results.  $\text{K}^+$  channels were not visible under the present experimental conditions (low  $[\text{K}^+]_o$ , see reference 18). The maximal number of channels simultaneously open throughout the recording ( $N_{\text{max}}$ ) was determined by a visual inspection. In cell-attached patches, the reversal potential of the  $i/v$  curve  $E_r$  is equal to the algebraic difference between  $E_m$  and the equilibrium potential for the ions passing through the channel. Relative ion permeabilities were estimated from the reversal poten-

tial for current flow ( $E_r$ ) using the voltage Goldman-Hodgkin-Katz equation.

The patch-pipette and bath solutions contained (mM): NaCl 140, KCl 4.8,  $\text{MgCl}_2$  1.2,  $\text{CaCl}_2$  1, glucose 10, Hepes 10 and were adjusted to pH 7.4 with NaOH. Bathing solutions used for inside-out patches were titrated to pH 7.2 and the  $\text{Ca}^{2+}$  concentration was usually brought to  $< 10^{-8}$  M by adding 2 mM EGTA. A low-NaCl solution differed from the standard solution in that the NaCl concentration was reduced to 14 mM (with 260 mM sucrose) and no KCl was included. The liquid-junction potential was determined using a 2.7 M KCl-filled pipette placed successively in control and low-NaCl solutions, and measuring the resulting voltage deflection in zero-current clamp. A value of 9 mV was found, and  $V_c$  was corrected accordingly. Experiments were conducted at room temperature (20–24°C) unless otherwise stated.

**Assessment of  $\text{Na}^+ - \text{K}^+ - 2\text{Cl}^-$  cotransport activity.** The activity of the  $\text{Na}^+ - \text{K}^+ - 2\text{Cl}^-$  cotransporter was monitored by taking advantage of the fact that  $\text{NH}_4^+$  can be taken up by the cotransporter in place of  $\text{K}^+$  (19, 20).  $\text{NH}_4\text{Cl}$  (4 mM) was superfused onto CTAL tubules, causing sustained intracellular acidification, which was preceded by a transient alkalization. The time courses of intracellular pH ( $\text{pH}_i$ ) decreases in the presence of  $\text{NH}_4\text{Cl}$  (see Fig. 7) were fitted by a one-exponential equation.  $\text{Na}^+ - \text{K}^+ - 2\text{Cl}^-$  cotransport activity was defined as the bumetanide-sensitive component of the acidification rate (20), i.e., the difference between acidification rates in the absence and

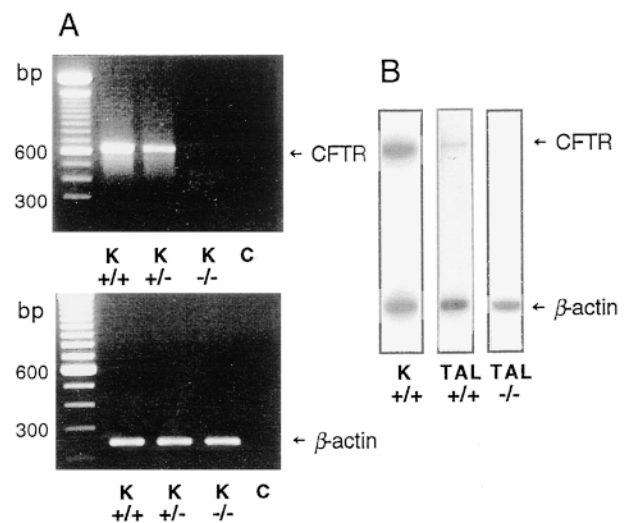


**Figure 1.** *CFTR* mRNA in whole kidney and microdissected CTAL. Total RNA was extracted from mouse whole kidneys and CTALs and was reverse-transcribed. (A) Samples of cDNA (300 ng) from whole kidneys (K) were amplified by PCR for 35 cycles. 15- $\mu\text{l}$  aliquots of the PCR reaction were loaded on a 2% agarose gel and the fragments were stained with ethidium bromide. (Top) Amplified products of the expected size (636 bp) were obtained in *CFTR* ( $+/+$ ) and *CFTR* ( $+/-$ ) mice with *CFTR* primers. No bands were detected in *CFTR* ( $-/-$ ) mice or by omitting cDNA (C). (Bottom) Equivalent amounts of amplified products (250 bp) for  $\beta$ -actin, used as internal standard, were detected using 300-ng aliquots from the same cDNAs of *CFTR* ( $+/+$ ), *CFTR* ( $+/-$ ), and *CFTR* ( $-/-$ ) mice. No bands were detected by omitting cDNA (C) or using non-reverse-transcribed RNA (not shown). (B) Autoradiograms of  $^{32}\text{P}$ -labeled fragments formed by RT-PCR from whole kidney of a *CFTR* ( $+/+$ ) mouse (K) and CTALs microdissected from *CFTR* ( $+/+$ ) [TAL  $+/+$ ] and *CFTR* ( $-/-$ ) [TAL  $-/-$ ] kidneys. *CFTR*-amplified products for 34 cycles from 100 ng cDNA were detected in the normal mouse kidney and in normal microdissected CTAL when compared with the amount of  $\beta$ -actin-amplified products. No *CFTR* mRNA was detected in *CFTR* ( $-/-$ ) CTAL.

presence of bumetanide. The activity of other  $\text{NH}_4^+$  transporters (19, 20) was reduced by including  $250 \mu\text{M Ba}^{2+}$  throughout the experiment.

BCECF fluorescence was monitored in ratio mode using video-enhanced fluorescence microscopy and image processing (Argus-50; Hamamatsu Photonics K.K., Hamamatsu City, Japan) at  $37^\circ\text{C}$ . A CTAL was epi-illuminated at 490 and 440 nm and the fluorescence emitted from a  $50\text{--}80\text{-}\mu\text{m}$  long portion of the CTAL was detected at 535 nm by an intensified CCD camera (C2400-87; Hamamatsu). Images were generated at each excitation wavelength by integrating eight frames ( $256 \times 241$  pixels). Image pairs, acquired every 20 s (control) or 3 s ( $\text{NH}_4\text{Cl}$  exposure), were ratioed on a pixel-by-pixel basis, and converted to  $\text{pH}_i$  values (10) using the high  $\text{K}^+$ /nigericin method (8). All fluorescent images were corrected for shading. Background noise (including cellular autofluorescence) was not detectable.

**Microperfusion experiments.** CTALs were microperfused *in vitro* (21). The tubule lengths in the three groups were not statistically different (not shown). Each tubule was transferred to a Lucite chamber kept at  $36.0 \pm 0.1^\circ\text{C}$ , with a flow rate of  $\sim 5$  ml/min, and allowed to equilibrate for 1 h. AVP ( $10^{-10}$  M) was added to the bath for 40 min after a 30-min control period. Samples of luminal fluid were collected every 10 min. The composition of the perfusion solution was (mM): NaCl 140, KCl 4,  $\text{Na}_2\text{HPO}_4$  0.33,  $\text{NaH}_2\text{PO}_4$  0.44,  $\text{MgCl}_2$  1,  $\text{MgSO}_4$  0.8,  $\text{CaCl}_2$  1, Hepes 10, and urea 10. Glucose (5 mM) was added to the bathing solution. All solutions were adjusted to pH 7.4.  $\text{Cl}^-$  concentrations in the collected fluid ( $C_c$ ) and perfusate ( $C_p$ ) were determined by microelectrometric titration. The flow rate ( $V$ ) was calculated from the volume of the collected sample, assuming that water reabsorption was negligible in these segments (1). The net  $\text{Cl}^-$  flux was calculated as  $J_{\text{Cl}} = (C_c - C_p)V$ , expressed in picomoles per minute.

**Statistics.** Experimental values are given as means  $\pm$  SEM;  $n$  denotes the number of experiments. Statistical significance was evaluated within each series by paired Student's  $t$  test. Data were compared between groups using one-way ANOVA or Kruskal-Wallis analysis when the data were not normally distributed (SigmaStat; SpSS GmbH, Erkrath, Germany). Proportions were compared using the  $\chi^2$  test. A  $P$  value of 0.05 was considered significant.

## Results

**CFTR mRNA in mouse kidney and thick ascending limb.** RT-PCR was used to detect CFTR mRNA in the whole kidney and microdissected CTALs. CFTR mRNA was detected in the kid-

neys from CFTR (+/+) and from CFTR (+/-) mice, but not in kidneys from CFTR (-/-) mice (Fig. 1 A). CTALs microdissected from CFTR (+/+) mouse kidneys showed CFTR transcripts but no CFTR mRNA was found in CFTR (-/-) CTALs (Fig. 1 B).

**Channel recording in cell-attached patches.** Previous studies showed that the CTAL basolateral membrane contains a  $\text{Cl}^-$  channel of  $\sim 9$  pS. This channel is readily detected in the cell-attached configuration when tubules are preincubated with a solution containing  $10 \mu\text{M}$  forskolin for at least 10 min (5, 8). The first series of experiments determined whether this channel was present in CTAL tubules microdissected from CFTR (-/-) mice. Cell-attached patches revealed an ion channel with a unit conductance of  $\sim 9$  pS in CFTR (+/+) ( $9.0 \pm 0.7$  pS,  $n = 16$ ), CFTR (+/-) ( $8.0 \pm 0.5$  pS,  $n = 31$ ), and CFTR (-/-) ( $8.8 \pm 0.3$  pS,  $n = 35$ ) mice. The reversal potential was close to 0 mV in the three groups, suggesting that the permeating ion species was at equilibrium [CFTR (+/+) :  $0.4 \pm 1.6$  mV,  $n = 16$ ; CFTR (+/-) :  $0.3 \pm 1.5$  mV,  $n = 31$ ; CFTR (-/-) :  $-0.3 \pm 1.1$  mV,  $n = 35$ ]. The unit conductances and reversal potentials for the three groups of CTAL tubules were not statistically different and were quite similar to those previously reported (5). The percentage of patches containing this channel was also similar in the three groups: 69% for CFTR (+/+) (29 patches from 15 mice), 79% for CFTR (+/-) (62 patches from 25 mice), and 78% for CFTR (-/-) (69 patches from 24 mice). Fig. 2 A shows openings of this channel obtained in the cell-attached mode from a CFTR (-/-) CTAL. Very brief openings of a second type of  $\text{Cl}^-$  channel (3) are visible in some instances. The mean  $i/v$  relationship of the small channel in the cell-attached mode is shown in Fig. 2 B for CFTR (-/-).

We then assessed the normalized current,  $NP_o$ , as an estimate of channel activity in cell-attached patches, using  $\text{NH}_4\text{Cl}$  superfusion to determine the closed current. Channel activity was recorded for 2–3 min at  $+80/+100$  mV. Then a solution containing  $10$  mM  $\text{NH}_4\text{Cl}$  was superfused onto the tubule.  $\text{NH}_4\text{Cl}$  caused an initial transient alkalization, followed by tonic intracellular acidification (see Fig. 6), and almost completely inhibited the 9-pS  $\text{Cl}^-$  channel, which is pH sensitive

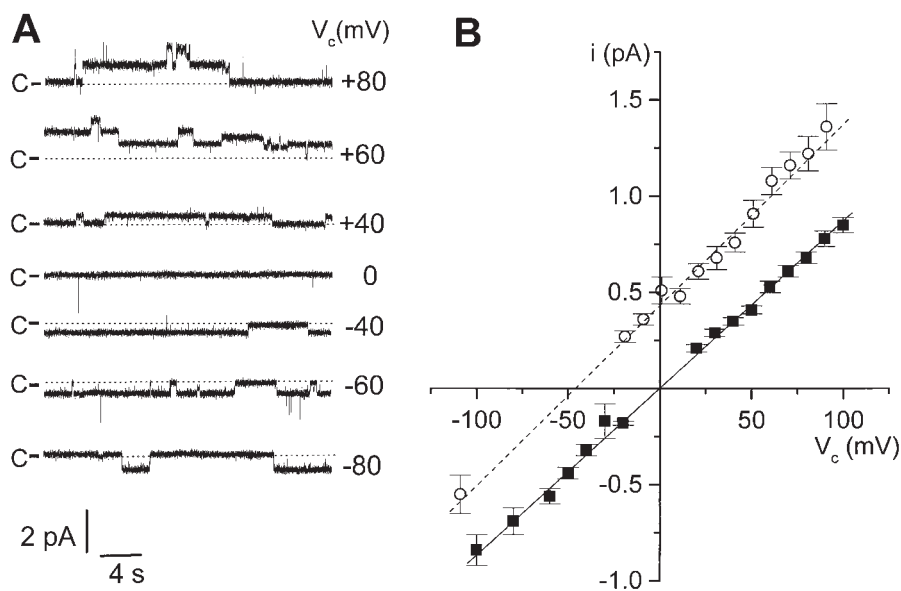


**Figure 2.** 9-pS  $\text{Cl}^-$  channel recorded from CTAL tubules of CFTR (-/-) mice. (A) Single-channel current recordings at various clamp potentials ( $V_c$ ) recorded from one basolateral membrane patch in the cell-attached configuration.  $V_c$  is superimposed on the spontaneous cell membrane potential (which is unknown). Some brief openings of a second type of  $\text{Cl}^-$  channel (3) are superimposed upon the smaller openings of the 9-pS  $\text{Cl}^-$  channel. Pipette and bath: 140 mM NaCl solution. The letter C to the left of the trace indicates the closed current level in this and subsequent figures. (B) Mean  $i/v$  relationships for the channel, obtained from CFTR (-/-) tubules in the cell-attached configuration (filled squares, bath: 140 mM NaCl solution, 8–30 measurements in 31 patches) and in the inside-out configuration (open circles, bath: 14 mM NaCl solution, 5–10 measurements in 12 patches). Pipette: NaCl solution. Points are means  $\pm$  SEM. The lines are linear regressions of the data.

(8). The mean current over the control period was measured taking the leak current value in the presence of  $\text{NH}_4\text{Cl}$  as baseline, and used to calculate  $NP_o$ . Fig. 3 A shows a current recording from a patch formed on a CFTR (+/-) tubule which contained a large number of channels.

$NP_o$  was very variable in each group, ranging from less than 1 to 110 (Fig. 3 B). This cannot be attributed to variations in pipette tip size, since we used pipettes with the same resistance (3.9–5.7 M $\Omega$ ) throughout the study. A plot of  $NP_o$  in each group showed no correlation with pipette resistance. Thus the variations in  $NP_o$  suggest that either the 9-pS  $\text{Cl}^-$  channels are distributed in clusters, or that the cells have widely differing  $\text{Cl}^-$  conductances. The mean  $NP_o$ s were  $32 \pm 8$  ( $n = 17$ ) for CFTR (+/+),  $27 \pm 7$  ( $n = 12$ ) for CFTR (+/-), and  $25 \pm 8$  ( $n = 16$ ) for CFTR (-/-) tubules (Fig. 3 B); they were not statistically different. The maximal numbers of small-conductance  $\text{Cl}^-$  channels ( $N_{\text{max}}$ ) in each patch for the three tubule groups

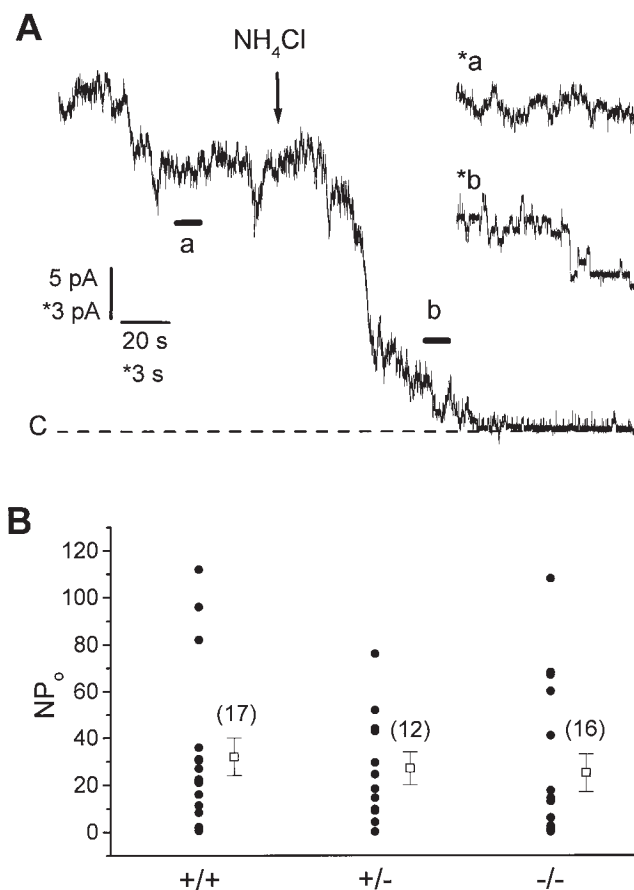


**Figure 3.** An estimate of the number of 9-pS  $\text{Cl}^-$  channels in cell-attached patches. (A) Current recording at +80 mV from a cell-attached patch formed on a CFTR (+/-) CTAL tubule. At the arrow, a NaCl solution containing 10 mM  $\text{NH}_4\text{Cl}$ , superfused onto the tubule to acidify the intracellular compartment, rapidly inhibited the activity of the 9-pS  $\text{Cl}^-$  channel, as previously reported (8). Taking the final current level as baseline, a  $NP_o$  of 42 was calculated for this particular patch. (Inset) Current recordings from the same cell-attached patch on an expanded time scale. Letters indicate the position of the excerpt within the continuous recording. (B) Histograms showing the distribution of  $NP_o$  in patches attached to CFTR (+/+), (+/-), and (-/-) CTALs. Mean  $NP_o \pm \text{SEM}$  (open squares) were not statistically different (ANOVA on ranks). Numbers of observations are shown in parentheses.

were also similar (data not shown). The experiments were repeated at 37°C in the absence of forskolin and gave qualitatively similar results: the small-conductance  $\text{Cl}^-$  channel was present in CFTR (-/-) tubules and had an  $N_{\text{max}}$  of  $12 \pm 3$  ( $n = 10$ ), whereas the  $N_{\text{max}}$  was  $18 \pm 5$  ( $n = 10$ ) in CFTR (+/+) and  $9 \pm 4$  ( $n = 9$ ) in CFTR (+/-) patches (NS, ANOVA on ranks).

**Conductance and selective properties of the channel in excised patches.** In the excised configuration, identical NaCl solutions on both sides of the membrane patch resulted in channels with similar conductances in CFTR (+/+), CFTR (+/-), and CFTR (-/-) CTALs (Table I, no statistical differences between the groups).

The anion/cation selectivity was determined by reducing the NaCl concentration in the bathing solution to 14 mM while keeping the pipette solution at 140 mM NaCl. The  $i/v$  curves for the channel from CFTR (+/+), CFTR (+/-), and CFTR (-/-) CTAL tubules were similar, the unit conductances were identical, and the reversal potentials were close to the equilibrium potential for chloride, verifying that the channel is chloride selective (see Table I). The reversal potentials were used to calculate a  $P_{\text{Cl}}/P_{\text{Na}}$  permeability ratio of 13.5–16.9 (Table I). Fig. 2 B shows the mean  $i/v$  relationship for CFTR (-/-) CTALs with a 14 mM NaCl bathing solution. Previously, we observed that replacing all  $\text{Cl}^-$  with  $\text{I}^-$  resulted in total inhibition of the channel (7). Therefore, we obtained an estimate of  $P_{\text{I}}/P_{\text{Cl}}$  by measuring the shift in the reversal potential when a 14 mM NaCl solution was supplemented with 10 mM NaI. This caused a 20-mV shift of the reversal potential towards positive voltages (Table I), showing that the channel is highly permeable to  $\text{I}^-$  ( $P_{\text{I}}/P_{\text{Cl}} \approx 2$ ) in all three tubule groups.

**Regulation in inside-out patches: effects of internal pH, ATP, and pyrophosphate.** The 9-pS  $\text{Cl}^-$  channel in CTAL is stimulated by internal ATP in ~30–60% of inside-out patches (5). Channel activity was stimulated by ATP in CFTR (-/-) CTAL tubules (Fig. 4 A). 1 mM ATP increased  $NP_o$  in 52% of patches from CFTR (+/+) tubules (21 test patches), 37% of patches from CFTR (+/-) tubules (27 test patches), and 30% of patches from CFTR (-/-) tubules (27 test patches). The changes in  $NP_o$  induced by ATP varied greatly, from 0.1 to 4.0, in each tubule group. The differences between groups for the percentage of responding patches and the increase in  $NP_o$  ( $\Delta NP_o$ ) were not statistically significant (Fig. 4 B).

Pyrophosphate stimulates the activity of the human CFTR  $\text{Cl}^-$  channel (22, 23). Pyrophosphate (5 mM) increased the  $NP_o$  of the 9-pS  $\text{Cl}^-$  channel to a similar extent in CFTR (+/+) and CFTR (-/-) CTALs in the presence of ATP:  $161 \pm 12$  ( $n = 3$ ) and 192% ( $n = 2$ ), respectively, when expressed as a percentage of control. A typical response for a CFTR (+/+) tubule is given in Fig. 4 C. Pyrophosphate had no effect when no channel was active in the ATP-containing solution.

One important property of the CTAL  $\text{Cl}^-$  channel that distinguishes it from the human recombinant CFTR channel (6, 7) is that it is very sensitive to internal pH (10). This property was preserved in the thick ascending limb of CFTR (-/-) mice (Fig. 5 A). The effects of internal pH on channel activity were investigated by comparing the  $NP_o$  at pH 6.8 and at pH 7.6. to control (pH 7.2); there was no statistically significant difference between the three tubule groups (Fig. 5 B).

To complete this study, we investigated whether disruption of the *cftr* gene indirectly affected the activity of another  $\text{Cl}^-$  transport system, the  $\text{Na}^+\text{-K}^+\text{-Cl}^-$  cotransporter, or the overall  $\text{Cl}^-$  transport across the CTAL epithelium.

Table I. Conductive Properties of the 9-pS Cl<sup>-</sup> Channel in Excised Patches

	Solution	CFTR (+/+)	CFTR (+/-)	CFTR (-/-)
<i>g</i> (pS)	140 NaCl	10.4±1.4 (6)	8.4±0.8 (12)	9.6±0.6 (12)
<i>g</i> (pS)	14 NaCl	10.8±0.7 (13)	10.8±0.4 (11)	10.5±0.6 (12)
<i>E<sub>r</sub></i> (mV)	14 NaCl	-43.7±1.7 (13)	-42.6±2.1 (11)	-41.2±3.3 (12)
<i>P<sub>Cl</sub></i> / <i>P<sub>Na</sub></i>	14 NaCl	16.9	15.9	13.5
<i>g</i> (pS)	14 NaCl + 10 NaI	11.0 (2)	10.8±0.2 (4)	10.2±0.4 (4)
<i>E<sub>r</sub></i> (mV)	14 NaCl + 10 NaI	-20.3±1.7 (3)	-19.0±2.1 (4)	-19.1±2.6 (4)
<i>P<sub>I</sub></i> / <i>P<sub>Cl</sub></i>	14 NaCl + 10 NaI	2.0	2.0	1.9

The unit conductance (*g*) and the reversal potential (*E<sub>r</sub>*) were estimated from a linear regression of individual *i/v* relationships. (*n*), number of observations. The various solutions mentioned are standard (140 NaCl), low-NaCl (14 NaCl), and low-NaCl supplemented with 10 mM NaI (14 NaCl + 10 NaI) solutions. The Cl<sup>-</sup> to Na<sup>+</sup> (*P<sub>Cl</sub>*/*P<sub>Na</sub>*) and I<sup>-</sup> to Cl<sup>-</sup> (*P<sub>I</sub>*/*P<sub>Cl</sub>*) permeabilities were deduced from the mean *E<sub>r</sub>* values using the Goldman-Hodgkin-Katz voltage equation. There was no statistical difference between the groups.

**Na<sup>+</sup>-K<sup>+</sup>-2Cl<sup>-</sup> cotransporter activity.** One CTAL tubule was superfused with a Ringer solution containing 4 mM NH<sub>4</sub>Cl with and without the cotransporter inhibitor bumetanide (0.1 mM). As previously reported (19), the bilateral addition of NH<sub>4</sub>Cl, without bumetanide, in the presence of barium, led to a small, very transient alkalinization<sup>2</sup> followed by tonic acidifi-

cation (Fig. 6). The acidification was greatly blunted by bumetanide (Fig. 6). Bumetanide-sensitive acidification rates in CFTR (+/+) (-0.46±0.1 pH units/min, nine tubules from six mice), CFTR (+/-) (-0.35±0.05 pH units/min, five tubules from three mice), and CFTR (-/-) (-0.35±0.07 pH units/min, six tubules from four mice) mice were not statistically different, indicating similar activities in the three groups.

2. The NH<sub>4</sub>Cl-induced initial alkalinizations reflect the basolateral entry of the membrane-permeant species, NH<sub>3</sub>, and its intracellular combination with H<sup>+</sup> to form NH<sub>4</sub><sup>+</sup>. Since both apical and basolateral membranes were exposed to NH<sub>4</sub>Cl, [NH<sub>3</sub>]<sub>o</sub> is constant. As NH<sub>4</sub><sup>+</sup> enters the cells and dissociates into NH<sub>3</sub> and H<sup>+</sup>, the newly formed NH<sub>3</sub> tends to increase [NH<sub>3</sub>]<sub>i</sub> above its equilibrium and readily leaves the cells. Because the diffusion of NH<sub>3</sub> is thought to be at a faster rate than NH<sub>4</sub><sup>+</sup> entry, it is not rate limiting in the secondary acidification.

**Cl<sup>-</sup> absorption in isolated, microperfused CTAL tubules.**

The *J<sub>Cl</sub>* under basal conditions were not significantly different in the three groups (Fig. 7 A): 37.8±5.5 pmol/min (*n* = 13) for CFTR (+/+), 27.4±4.8 pmol/min (*n* = 12) for CFTR (+/-), and 26.0±4.9 pmol/min (*n* = 12) for CFTR (-/-) mice. The tubule perfusion rates, and hence the perfused chloride bulks for all the groups (Fig. 7 A), were also similar: 3.55±0.45, 3.28±0.27, and 3.21±0.55 nl/min for CFTR (+/+), CFTR (+/-),

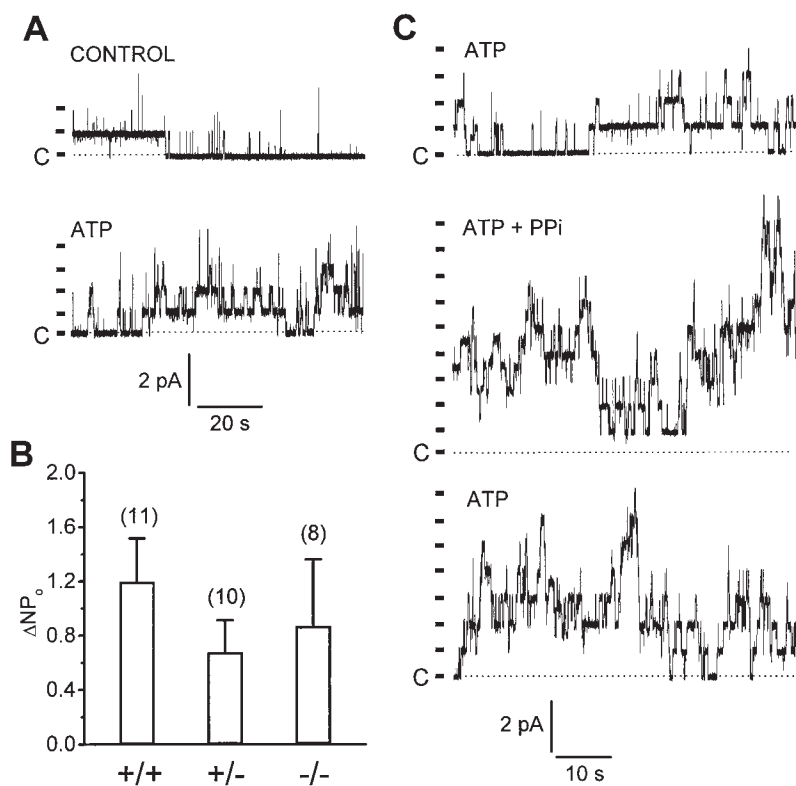
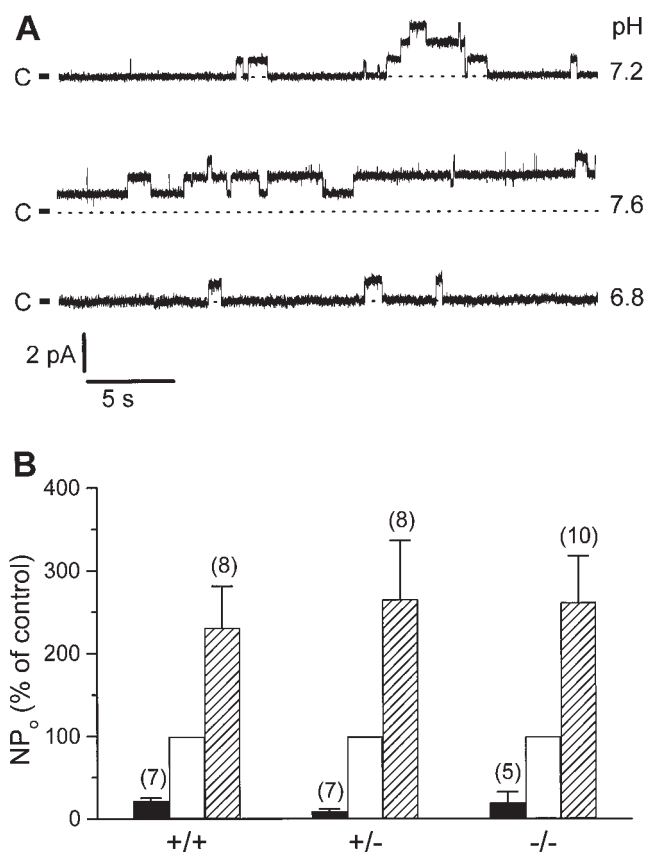


Figure 4. Activation of the 9-pS Cl<sup>-</sup> channel by internal ATP and by pyrophosphate. (A) Channel current recording from one inside-out patch in CFTR (-/-) tubule showing activation of the Cl<sup>-</sup> channel by ATP which is in the typical range for this group. The large, brief deflections are openings of the second type of Cl<sup>-</sup> channel with a larger conductance (3). *V<sub>c</sub>* = 59 mV. (B) Histograms showing the increase in *NP<sub>o</sub>* ( $\Delta NP_o$ ) induced by 1 mM ATP. Numbers of observations are shown in parentheses. The data were not different between groups (ANOVA on ranks).  $\Delta NP_o$  values were 1.2±0.3 for CFTR (+/+), 0.7±0.2 for CFTR (+/-), and 0.9±0.5 for CFTR (-/-) CTALs. (C) Current recording from one inside-out patch formed on a CFTR (-/-) CTAL showing the activation of the 9-pS Cl<sup>-</sup> channel by pyrophosphate (PPi, 5 mM) in the presence of ATP. Inside-out patches were bathed with a 14 mM NaCl solution (pipette: NaCl solution). *V<sub>c</sub>* = 69 mV.



**Figure 5.** Modulation of  $\text{Cl}^-$  channel activity by internal pH. (A) Current recording traces from one inside-out patch formed on a CFTR (-/-) CTAL bathed with a 14 mM NaCl solution (pipette: 140 mM NaCl solution) at pH 7.2, 7.6, and 6.8.  $V_c = 50$  mV. (B) Histograms giving  $\text{NP}_o$  at pH 7.6 (hatched bars) and pH 6.8 (filled bars), expressed in percentages of  $\text{NP}_o$  at pH 7.2 (open bars), for the three tubule groups. There were no differences between the groups in the results obtained at pH 7.6 (ANOVA) or at pH 6.8 (ANOVA on ranks).

and CFTR (-/-) mice, respectively. There was also a significant linear relationship between  $J_{\text{Cl}}$  and the flow rate for the CFTR (-/-) and CFTR (+/+) groups ( $y = 9.6x - 2.5$ ,  $P < 0.001$ , and  $y = 9.0x + 3.1$ ,  $P < 0.01$ , respectively). But there were no significant differences in the slopes and ordinates, indicating that  $J_{\text{Cl}}$  was not different in the two groups for a similar tubule flow rate (Fig. 7 B).

The effect of AVP on  $J_{\text{Cl}}$  was investigated in the three groups of mice, since this hormone increases the intracellular cyclic AMP in the mouse TAL (21). The AVP effect was not tested in two tubules from CFTR (-/-) mice. The hormone significantly increased  $J_{\text{Cl}}$  by  $17.1 \pm 5.1$  pmol/min for the CFTR (+/+),  $16.5 \pm 2.6$  pmol/min for CFTR (+/-), and  $17.0 \pm 5.3$  pmol/min for CFTR (-/-) mice (Fig. 7 C). The data from the three groups (Fig. 7 D) fitted the same linear relationship between  $J_{\text{Cl}}$  values in the presence and absence of AVP ( $y = 1.3x + 7.9$ ,  $r = 0.89$ ,  $P < 0.001$ ).

## Discussion

This study on *cftr<sup>tm1Unc</sup>* mice (10) shows that the 9-pS CTAL  $\text{Cl}^-$  channel is present at the same frequency in cell-attached patches from CFTR (+/+), CFTR (+/-), and CFTR (-/-)

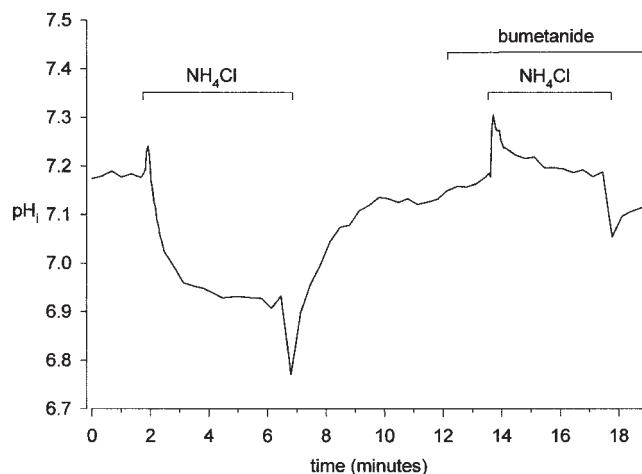


**Figure 6.**  $\text{Na}^+$ - $\text{K}^+$ - $2\text{Cl}^-$  cotransport activity in a CFTR (-/-) CTAL. The tubule was continuously superfused with Ringer's solution containing  $250 \mu\text{M}$   $\text{BaCl}_2$  and exposed to 4 mM  $\text{NH}_4\text{Cl}$  in the absence and presence of  $100 \mu\text{M}$  bumetanide. Least-squares fitting of the time courses of the  $\text{pH}_i$  decrease caused by  $\text{NH}_4\text{Cl}$  gave acidification rates of  $-0.64$  in the absence of bumetanide and  $-0.18$  pH unit/min in its presence. Similar values were found for CFTR (+/+) and CFTR (+/-) mice.

mice. It has the same ion selectivity properties and similar sensitivities to pH, ATP, and pyrophosphate in all three groups of mice. In addition, the overall  $\text{Cl}^-$  absorption across CTAL epithelium is normal in CFTR (-/-) mice.

**The 9-pS CTAL  $\text{Cl}^-$  channel and CFTR.** Several lines of evidence indicate that the CTAL  $\text{Cl}^-$  channel is distinct from CFTR. First, the currents due to 9-pS channel activity were similar in CFTR (-/-), CFTR (+/+), and CFTR (+/-) mice. The only published single-channel study of *cf* mice found that there were few CFTR  $\text{Cl}^-$  channels in the apical membrane of cultured gall bladder cells from a  $\Delta\text{F508}$  cystic fibrosis mouse (24): the number of channels per patch was 16% of that in normal mice at room temperature. Because the processing of  $\Delta\text{F508}$  protein may be facilitated at room temperature (2), the authors also tested for the presence of the mutated CFTR at 37°C and reported that the number of CFTR channels per patch was 1% of that in normal mice at this temperature. A similar loss of CFTR should be expected in our study if the CTAL channel was a CFTR protein.

The same studies (24) indicated that the mouse CFTR has a lower unit conductance ( $\sim 5$  pS) than the CTAL  $\text{Cl}^-$  channel (8–10 pS). Recently, a similar unit conductance of 5.8 pS was found at 37°C for mouse CFTR expressed in Chinese hamster ovary cells (25). We find that the unit conductance of the CTAL  $\text{Cl}^-$  channel is  $\sim 11$ –12 pS at 37°C [CFTR (+/+):  $12.6 \pm 0.8$  pS ( $n = 10$ ); CFTR (+/-):  $11.1 \pm 0.9$  pS ( $n = 10$ ); CFTR (-/-):  $11.9 \pm 0.6$  pS ( $n = 11$ )]. The human CFTR (6, 7) is also rather insensitive to pH (this characteristic has not been investigated in the mouse), whereas the CTAL  $\text{Cl}^-$  channel is very sensitive to internal pH (8). There are other, additional differences: the  $\text{I}^-$  to  $\text{Cl}^-$  permeability ratio (deduced from reversal potentials in inside-out patches) is  $> 1$  in both the mouse and the human CFTR (24, 26), as it is in CTAL  $\text{Cl}^-$  channel (5). However, interaction of  $\text{I}^-$  with the channel pore reduces the unit conductance in CFTR (24, 26), whereas it decreases  $P_o$  in the TAL  $\text{Cl}^-$  channel without decreasing the unit

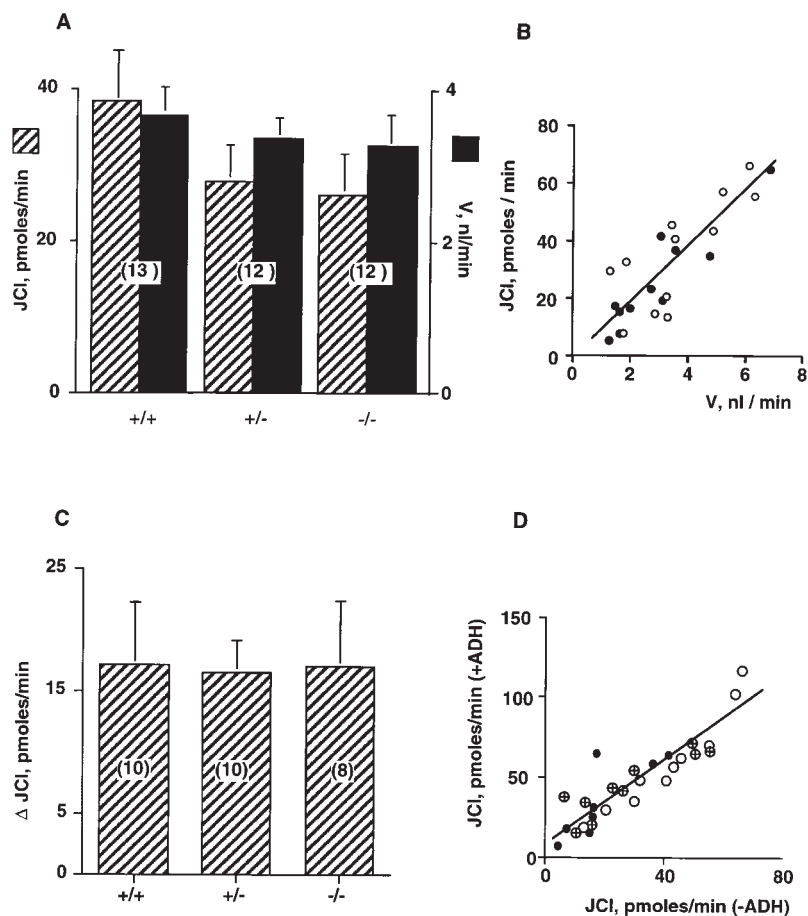


Figure 7. Net  $Cl^-$  absorption in CTAL tubules. (A) Net  $Cl^-$  absorption ( $J_{Cl}$ , hatched bars) and tubule perfusion rate ( $V$ , filled bars). Numbers of tubules are shown in parentheses. (B) Curve describing the linear relationship between  $J_{Cl}$  (ordinate) and the flow rate (abscissa) in CFTR (-/-) (filled circles) and CFTR (+/+) (open circles) mice. One point was discarded from each of the two groups. The equation was  $y = 9.5x - 0.45$ ,  $r = 0.85$ ,  $P < 0.001$ , for the pooled data from the two groups. There was no significant linear relationship for CFTR (+/-) mice. (C) Net difference in  $J_{Cl}$  ( $\Delta J_{Cl}$ ) in the presence and absence of AVP, on the same tubule. (D) Curve describing the linear relationship between the net  $Cl^-$  flux in the presence (ordinate) and in the absence (abscissa) of AVP for CFTR (+/+) (open circles), CFTR (+/-) (crossed circles), and CFTR (-/-) (filled circles) mice. The equation was  $y = 1.3x + 7.9$ ,  $r = 0.89$ ,  $P < 0.001$ , for the pooled data from the three groups.

conductance (5). Pyrophosphate moderately stimulates the activity of the CTAL  $Cl^-$  channel, whereas it has no effect on mouse CFTR (25), but does not lock open the CTAL  $Cl^-$  channel as it does for the human CFTR (22, 23).

The CFTR protein has been located in the human and rat renal tubule by immunocytochemistry. It is in the apical membranes of human distal tubule (27) and the rat cortical collecting tubule (28), but there has been no report of CFTR in the TAL basolateral membranes. The CFTR seems to be restricted to the cytoplasmic compartment in TAL as in the proximal tubule (28).

*Cl<sup>-</sup> absorption in isolated CTAL tubules from cf mice.* An important finding of this study is that the  $Cl^-$  absorption across the TAL segment is not altered in the basal state in *cf* mice and remains sensitive to stimulation by vasopressin via cAMP. In contrast, there is no detectable cAMP-dependent  $Cl^-$  secretion in the intestine, airways, or pancreas in this *cf* model (11–15 and this study, see Methods). These results are in accordance with what is expected from a mouse model of cystic fibrosis. There are no striking disturbances of renal function in patients with cystic fibrosis, although there have been a few reports of alterations, such as a decrease in the dilution capacity (see reference 29).

It was reported recently that the sensitivity of the renal  $K^+$  channel, ROMK2, to glibenclamide is enhanced by coexpression with CFTR (30). This type of channel in the TAL apical membrane modulates NaCl absorption by recycling the  $K^+$  ions transported into the cell by the  $Na^+K^+-2Cl^-$  cotransporter and by participating in the setting of the transepithelial

potential difference (1). Our results suggest that the functioning of this  $K^+$  channel is not altered in CFTR (-/-) mice, at least as far as  $K^+$  recycling is concerned. However, many regulatory possibilities of CFTR were not explored in this study, leaving open the question of the physiological role of CFTR in TAL.

*The molecular nature of the 9-pS CTAL Cl<sup>-</sup> channel.* Our results indicate that the 9-pS CTAL  $Cl^-$  channel is distinct from CFTR. Several properties of the channel, notably stimulation by ATP, PKA, and pyrophosphate, strongly suggest a structural similarity with CFTR and hence the ATP binding cassette proteins. Vankuijck et al. (31) have reported the cloning of a cAMP-activated chloride conductance regulator (epithelial basolateral chloride conductance regulator, EBCR) belonging to the ATP-binding cassette family. Antibodies detected the EBCR on the basolateral side of TALs and distal tubules of rabbit kidney (31). The protein generates  $Cl^-$  currents which are activated by cAMP and blocked by 5-nitro-2-(3-phenylpropylamino)benzoic acid, niflumic acid, and DIDS (31) in oocytes. However, it is unclear whether the protein itself is a channel or if it acts as a modulator of endogenous  $Cl^-$  channels. Further investigation is needed to determine whether EBCR, alone or associated with another  $Cl^-$  channel, participates in the CTAL basolateral  $Cl^-$  conductance. The renal tubule contains CIC  $Cl^-$  channels (see reference 32) that could be involved in the formation of the 9-pS  $Cl^-$  channel. One human homologue to CIC-K1, CICNKB, was found recently to cause a new type of Bartter's syndrome, thus pointing to the importance of CIC  $Cl^-$  channels in the TAL segment (33).

## Acknowledgments

We thank M.-F. Bertrand (CDTA, Orléans, France) for her help throughout this study and C. Rozé (Paris, France) for making available a short-circuit current measuring device. The English text was corrected by O. Parkes.

This work was funded by INSERM, CNRS, the Fondation pour la Recherche Médicale (FRM), and by the Association Française de Lutte contre la Mucoviscidose (AFLM). P. Marvão was the recipient of a fellowship from INSERM and R. Guinamad was supported by FRM.

## References

1. Reeves, W.B., and T.E. Andreoli. 1992. Sodium chloride transport in the loop of Henle. In *The Kidney: Physiology and Pathophysiology*. D.W. Seldin and G. Giebisch, editors. Raven Press, New York. 1975–2001.
2. Welsh, M.J. 1996. Cystic fibrosis. In *Molecular Biology of Membrane Transport Disorders*. S.G. Schultz, editor. Plenum Press, New York. 605–623.
3. Paulais, M., and J. Teulon. 1990. A cAMP-activated chloride channel in the basolateral membrane of the thick ascending limb of the mouse kidney. *J. Membr. Biol.* 113:253–260.
4. Winters, C.J., W.B. Reeves, and T.E. Andreoli. 1990. Cl<sup>-</sup> channels in basolateral renal medullary membranes. III. Determinants of single-channel activity. *J. Membr. Biol.* 118:269–278.
5. Guinamad, R., A. Chraïbi, and J. Teulon. 1995. A small-conductance Cl<sup>-</sup> channel in the mouse thick ascending limb that is activated by ATP and protein kinase A. *J. Physiol. (Lond.)*. 485:97–112.
6. Sheppard, D.N., and K.A. Robinson. 1997. Mechanism of glibenclamide inhibition of cystic fibrosis transmembrane conductance regulator Cl<sup>-</sup> channels expressed in a murine cell line. *J. Physiol. (Lond.)*. 503:333–346.
7. Sherry, A.M., J. Cupoletti, and D.H. Malinowska. 1994. Differential acidic pH sensitivity of ΔF 508 CFTR Cl<sup>-</sup> channel activity in lipid bilayers. *Am. J. Physiol.* 266:C870–C875.
8. Guinamad, R., M. Paulais, and J. Teulon. 1995. Inhibition of a small-conductance cAMP-dependent Cl<sup>-</sup> channel in the mouse thick ascending limb at low internal pH. *J. Physiol. (Lond.)*. 490:759–765.
9. Morales, M.M., T.P. Carroll, T. Morita, E.M. Schwiebert, O.M. Devuyst, P.D. Wilson, A.G. Lopes, B.A. Stanton, H.C. Dietz, G.R. Cutting, and W.B. Guggino. 1996. Both the wild type and a functional isoform of CFTR are expressed in kidney. *Am. J. Physiol.* 270:F1038–F1048.
10. Snouwaert, J.N., K.K. Brigman, A.M. Latour, N.N. Malouf, R.C. Boucher, O. Smithies, and B.H. Koller. 1992. An animal model for cystic fibrosis made by gene targeting. *Science*. 257:1083–1088.
11. Clarke, L.L., B.R. Grubb, S.E. Gabriel, O. Smithies, B.H. Koller, and R.C. Boucher. 1992. Defective epithelial chloride transport in a gene-targeted mouse model of cystic fibrosis. *Science*. 257:1125–1128.
12. Grubb, B.R. 1995. Ion transport across the jejunum in normal and cystic fibrosis mice. *Am. J. Physiol.* 268:G505–G513.
13. Leung, A.-Y.H., P.Y. Wong, S.E. Gabriel, J.R. Yankaskas, and R.C. Boucher. 1995. cAMP- but not Ca<sup>2+</sup>-regulated Cl<sup>-</sup> conductance in the oviduct is defective in mouse model of cystic fibrosis. *Am. J. Physiol.* 268:C708–C712.
14. Clarke, L.L., B.R. Grubb, J.R. Yankaskas, C.U. Cotton, A. McKenzie, and R.C. Boucher. 1994. Relationship of a non-cystic fibrosis transmembrane conductance regulator-mediated chloride conductance to organ-level disease in Cfr(-/-) mice. *Proc. Natl. Acad. Sci. USA*. 91:479–483.
15. Grubb, B.R., A.M. Paradiso, and R.C. Boucher. 1994. Anomalies in ion transport in CF mouse tracheal epithelium. *Am. J. Physiol.* 267:C293–C300.
16. Duong Van Huyen, J.-P., M. Bens, and A. Vandewalle. 1998. Differential effects of aldosterone and vasopressin on chloride fluxes in transimmortalized mouse cortical collecting duct cells. *J. Membr. Biol.* 164:79–90.
17. Hamill, O., A. Marty, E. Neher, B. Sakmann, and F. Sigworth. 1981. Improved patch-clamp technique for high resolution recording from cells and cell-free membrane patches. *Pflügers Archiv Eur. J. Physiol.* 391:85–100.
18. Parent, L., J. Cardinal, and R. Sauvé. 1988. Single-channel analysis of a K channel at basolateral membrane or rabbit proximal tubule. *Am. J. Physiol.* 254:F105–F113.
19. Kikeri, D., A. Sun, M.L. Zeidel, and S.C. Hebert. 1989. Cell membranes impermeable to NH<sub>3</sub>. *Nature*. 339:478–480.
20. Amlal, H., C. Legoff, C. Vernimmen, M. Paillard, and M. Bichara. 1996. Na<sup>+</sup>-K<sup>+</sup>-Cl<sup>-</sup> cotransport in medullary thick ascending limb: control by PKA, PKC and 20-HETE. *Am. J. Physiol.* 271:C455–C463.
21. Bailly, C., M. Imbert-Teboul, N. Roinel, and C. Amiel. 1990. Isoproterenol increases Ca, Mg and NaCl reabsorption in mouse thick ascending limb. *Am. J. Physiol.* 258:F1224–F1231.
22. Carson, M.R., M.C. Winter, S.M. Travis, and M.J. Welsh. 1995. Pyrophosphate stimulates wild-type and mutant cystic fibrosis transmembrane conductance regulator Cl<sup>-</sup> channels. *J. Biol. Chem.* 270:20466–20472.
23. Gunderson, K.L., and R.R. Kopito. 1994. Effects of pyrophosphate and nucleotides analogs suggest a role for ATP hydrolysis in cystic fibrosis transmembrane conductance regulator channel gating. *J. Biol. Chem.* 269:19349–19353.
24. French, P.J., J.H. Van Doornick, R.H.P.C. Peters, E. Verbeek, N.A. Ameen, C.R. Marino, H.R. de Jonge, J. Bijman, and B.J. Scholte. 1996. A ΔF508 mutation in mouse cystic fibrosis transmembrane conductance regulator results in a temperature-sensitive processing defect in vivo. *J. Clin. Invest.* 98:1304–1312.
25. Lansdell, K.A., S.J. Delaney, D.P. Lunn, S.A. Thomson, D.N. Sheppard, and B.J. Wainwright. 1998. Comparison of the gating behaviour of human and murine cystic fibrosis transmembrane conductance regulator Cl<sup>-</sup> channels expressed in mammalian cells. *J. Physiol. (Lond.)*. 508:379–392.
26. Tabcharani, J.A., P. Linsdell, and J.W. Hanrahan. 1997. Halide permeation in wild-type and mutant cystic fibrosis transmembrane conductance regulator chloride channels. *J. Gen. Physiol.* 110:341–354.
27. Crawford, I., P.C. Maloney, P.L. Zeitlin, W.B. Guggino, S.C. Hyde, H. Turley, K.C. Gatter, A. Harris, and C.F. Higgins. 1991. Immunocytochemical localization of the cystic fibrosis product CFTR. *Proc. Natl. Acad. Sci. USA*. 88:9262–9266.
28. Devuyst, O.M., C.M. Burrow, E.M. Schwiebert, W.B. Guggino, and P.D. Wilson. 1996. Developmental regulation of CFTR expression during human nephrogenesis. *Am. J. Physiol.* 271:F723–F735.
29. Stanton, B.A. 1997. Cystic fibrosis transmembrane conductance regulator (CFTR) and renal function. *Wien Klinische Wochenschrift*. 109:457–464.
30. McNicholas, C.M., W.B. Guggino, E.M. Schwiebert, S.C. Hebert, G. Giebisch, and M.E. Egan. 1996. Sensitivity of a renal K<sup>+</sup> channel (ROMK2) to the inhibitory sulfonylurea compound glibenclamide is enhanced by coexpression with the ATP-binding cassette transporter cystic fibrosis transmembrane conductance regulator. *Proc. Natl. Acad. Sci. USA*. 93:8083–8088.
31. Vankuijck, M.A., R.A.M.H. Vanaubel, A.E. Busch, F. Lang, F.G.M. Russel, R.J.M. Bindels, C.H. Vanos, and P.M.T. Deen. 1996. Molecular cloning and expression of a cyclic AMP-activated chloride conductance regulator: a novel ATP-binding cassette transporter. *Proc. Natl. Acad. Sci. USA*. 93:5401–5406.
32. Fong, P., and T.J. Jentsch. 1995. Molecular basis of epithelial channels. *J. Membr. Biol.* 144:189–197.
33. Simon, D.B., R.S. Bindra, T.A. Mansfield, C. Nelson-Williams, E. Mendonca, R. Stones, S. Schurman, A. Nayir, H. Alpay, A. Bakkaaloglu, et al. 1997. Mutations in the chloride channel gene, CLCNKB, cause Bartter's syndrome type III. *Nat. Genet.* 17:171–178.